Continuum Mech. Thermodyn. (2010) 22:515–530
DOI 10.1007/s00161-010-0141-1

ORIGINAL ARTICLE

Shaohua Chen · Huajian Gao

Dynamic behaviors of mode III interfacial crack under a constant loading rate

Received: 30 March 2010 / Accepted: 3 May 2010 / Published online: 25 June 2010

Abstract In an earlier study on intersonic crack propagation, Gao et al. (J. Mech. Phys. Solids **49**: 2113–2132, 2001) described molecular dynamics simulations and continuum analysis of the dynamic behaviors of a mode II dominated crack moving along a weak plane under a constant loading rate. The crack was observed to initiate its motion at a critical time after the onset of loading, at which it is rapidly accelerated to the Rayleigh wave speed and propagates at this speed for a finite time interval until an intersonic daughter crack is nucleated at a peak stress at a finite distance ahead of the original crack tip. The present article aims to analyze this behavior for a mode III crack moving along a bi-material interface subject to a constant loading rate. We begin with a crack in an initially stress-free bi-material subject to a steadily increasing stress. The crack initiates its motion at a critical time governed by the Griffith criterion. After crack initiation, two scenarios of crack propagation are investigated: the first one is that the crack moves at a constant subsonic velocity; the second one is that the crack moves at the lower shear wave speed of the two materials. In the first scenario, the shear stress ahead of the crack tip is singular with exponent $-1/2$, as expected; in the second scenario, the stress singularity vanishes but a peak stress is found to emerge at a distance ahead of the moving crack tip. In the latter case, a daughter crack supersonic with respect to the softer medium can be expected to emerge ahead of the initial crack once the peak stress reaches the cohesive strength of the interface.

Keywords Mode III interfacial crack · Constant loading rate · Subsonic · Supersonic · Daughter crack

1 Introduction

It is a great pleasure for us to contribute to this special issue on the occasion of the 80th Birthday of Prof. Leonid I. Slepyan who has made many important contributions to dynamic fracture mechanics, as exemplified by his pioneering study in analytical solution techniques with lattice models of dynamic fracture [41,55], as well as his numerous recent contributions to this subject [46,56–59]. During the last three decades, problems of dynamic crack propagation in a homogeneous medium or along an interface between dissimilar materials have also been studied by many other authors, both theoretically and experimentally [2,9,13,17,19,20,24,38,54,30,60,16,18,26,27,31–33,50,51,62,11,14,15,29,36,37]. Many other studies on the dynamic behaviors of crack motion can be found in the monograph by [20]. From these studies, it is known that the attainable crack speed critically depends on the cracking mode.

Communicated by Dr. Lev Truskinovsky.

S. Chen (✉)
LNM, Institute of Mechanics, Chinese Academy of Sciences, Beijing 100190, China
E-mail: Chenshaohua72@hotmail.com

H. Gao
Division of Engineering, Brown University, Providence, RI 02912, USA
E-mail: Huajian_Gao@brown.edu

For mode III cracks in a homogeneous solid, only subsonic crack propagation is thought to be possible. For mode I cracks in a homogeneous solid, the physically admissible stress singularity and the energy release rate vanish for all crack velocities above the Rayleigh wave speed, rendering a forbidden zone that covers the complete intersonic and supersonic regimes in a linear elastic solid. A mode II crack faces a forbidden velocity zone between the Rayleigh and shear wave speeds. Other than this forbidden zone, a mode II crack is allowed to propagate in both sub-Rayleigh and super-shear velocity regimes. The limiting speed for a mode II crack is the Rayleigh wave speed only if the forbidden velocity zone is impenetrable. The mechanism by which a shear crack could jump from sub-Rayleigh to super-shear velocities has been studied by many researchers [3,6–8,23,25,39,40,47,48,52,53]. It has been found that the energy release rate is strictly zero at the Rayleigh wave speed, but a positive peak of shear stress developing at the shear wave front ahead of the crack tip could induce a microcrack, or a daughter crack, that moves at speeds exceeding the shear wave speed.

Recent studies have also been directed at combined atomistic-continuum studies of dynamic crack propagation along bi-material interfaces. Buehler and Gao [10] found that interface crack motion under large tensile loading can reach the Rayleigh wave speed of the stiffer material via nucleation of a daughter crack ahead of the initial (mother) crack, and that interface crack motion under shear-dominated loading can reach the longitudinal wave speed of the stiffer material by a mother–daughter–granddaughter mechanism that involves a sequential nucleation events of one generation of (mother) cracks giving birth to the next generation (daughter) cracks to overcome multiple speed barriers as an initially static interface crack is accelerated toward its ultimate limiting speed. These results are also largely consistent with other theoretical [42] as well as experimental results [49].

A logical extension of the above studies is that the limiting speed for a mode III interface crack should be the shear wave speed of the stiffer material, with daughter/granddaughter crack mechanisms to overcome possible intermediate speed barriers as an initial static crack is accelerated toward this limiting speed. This assertion will be studied and confirmed in the present study. We point out that a number of fundamental solutions for dynamic mode III interface cracks have been obtained by several authors [34,35,43,63]. Motivated by the set up of molecular dynamics simulations of crack propagation [3–5,12,10,11], we will consider an initially static mode III interface crack subject to a steadily increasing load which eventually leads to the initiation of dynamic crack motion and nucleation of a daughter crack to break through the first sound barrier. We will show that the results of this analysis are fully consistent with what would be expected based on previous studies on cracks under mode I and mode II loading conditions.

2 Description of the problem

Consider a bimaterial system composed of two homogeneous, isotropic, and linearly elastic solids. Materials 1 and 2 occupy the lower and upper half-planes, respectively. A semi-infinite crack lying along the interface of the bimaterial is initially stress-free and at rest. At time $t = 0$, the nominal shear stress is assumed to increase at a constant rate of $\dot{\tau}_0$. At time $t = t_{\text{init}}$, the crack suddenly starts to propagate along the bimaterial interface at a constant speed v, as shown in Fig. 1.

The deformation field can be decomposed into the following two sub-problems. First, a uniform deformation field corresponding to the constant loading rate $\dot{\tau}_0$ is applied in the same bimaterial without the crack; the initial velocity field is consistent with $\dot{\tau}_0$ such that there are no waves from the remote field, and the shear stress continues to rise in time as

$$\tau_{yz} = \dot{\tau}_0 t. \tag{1}$$

The second sub-problem has a constant shear traction $\dot{\tau}_0 t$ imposed on the crack faces (including the new ones generated by crack propagation) in order to negate the crack-face tractions from the first sub-problem. There is no initial velocity field. The crack tip remains stationary until a critical time, $t = t_{\text{init}}$, is reached at which the Griffith criterion is met. The crack tip then starts to propagate along the interface of the bimaterial.

3 General solutions for a propagating crack with a constant velocity

First, consider the fundamental problem of a mode III interface crack moving with a constant velocity v, which is less than the smaller shear wave speed of the two materials. A uniformly distributed antiplane shear traction $\dot{\tau}_0 t$ is applied on the original crack faces as well as the new ones generated by crack propagation.

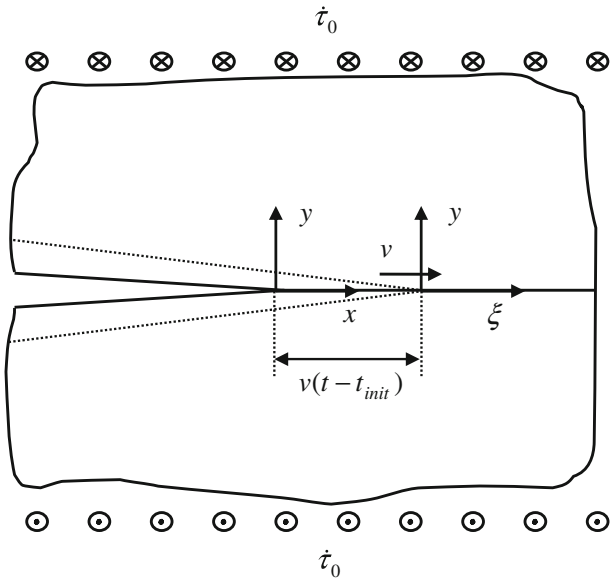

Fig. 1 Configuration and coordinate systems of a mode III interface crack subjected to a constant loading rate $\dot{\tau}_0$. Coordinate system (x, y) is fixed at the initial stationary crack tip and coordinate system (ξ, y) moves with the crack tip after initiation. The crack is stationary at time $t = 0$ and propagates at a velocity v after a critical time of initiation t_{init}

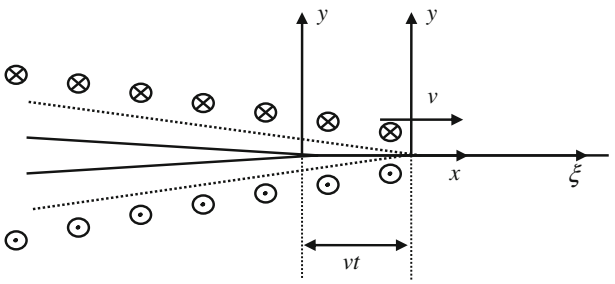

Fig. 2 Configuration and coordinate systems of a crack propagating along a bimaterial interface. A shear loading with a constant rate of increment is applied on the entire crack surface (including the newly created surfaces due to crack propagation)

Figure 2 shows the interface crack geometry and the coordinate systems. Materials 1 and 2 occupy the two half-spaces. The coordinate ξ is fixed with respect to the moving crack tip,

$$\xi = x - vt, \tag{2}$$

where we assume $v < C_{s1} < C_{s2}$, C_{si} $(i = 1, 2)$ denotes the shear wave speeds of the two materials and the subscript i $(i = 1, 2)$ refers to the lower and upper media, respectively.

In order to analyze this problem, it is convenient to express the governing equations of wave motions in the moving coordinates $\xi - y$ as follows [20]

$$\begin{cases} \left(1 - \frac{v^2}{C_{s1}^2}\right) \frac{\partial^2 w_1}{\partial \xi^2} + \frac{\partial^2 w_1}{\partial y^2} + \frac{2v}{C_{s1}^2} \frac{\partial^2 w_1}{\partial \xi \partial t} - \frac{1}{C_{s1}^2} \frac{\partial^2 w_1}{\partial t^2} = 0 \\ \left(1 - \frac{v^2}{C_{s2}^2}\right) \frac{\partial^2 w_2}{\partial \xi^2} + \frac{\partial^2 w_2}{\partial y^2} + \frac{2v}{C_{s2}^2} \frac{\partial^2 w_2}{\partial \xi \partial t} - \frac{1}{C_{s2}^2} \frac{\partial^2 w_2}{\partial t^2} = 0 \end{cases}, \tag{3}$$

in which w_i $(i = 1, 2)$ are the out-of-plane displacements in the two materials. The non-vanishing shear stresses are

$$\tau_{yzi} = \mu_i \frac{\partial w_i}{\partial y}, \quad \tau_{xzi} = \mu_i \frac{\partial w_i}{\partial x}, \tag{4}$$

where μ_i $(i = 1, 2)$ are the shear moduli of the two materials.

Using one-sided Laplace transform with respect to time t and two-sided Laplace transform with respect to ξ [20],

$$\hat{w}_i(\xi, y, s) = \int_0^\infty w_i(\xi, y, t)e^{-st}\mathrm{d}t, \tag{5}$$

$$W_i(\varsigma, y, s) = \int_{-\infty}^\infty \hat{w}_i(\xi, y, s)e^{-s\xi\varsigma}\mathrm{d}\xi, \tag{6}$$

the governing Eq. 3 become

$$\begin{cases} \left(1 - \frac{v^2}{C_{s1}^2}\right)s^2\zeta^2 W_1 + \frac{\partial^2 W_1}{\partial y^2} + \frac{2vs^2}{C_{s1}^2}\varsigma W_1 - \frac{s^2}{C_{s1}^2}W_1 = 0 \\ \left(1 - \frac{v^2}{C_{s2}^2}\right)s^2\zeta^2 W_2 + \frac{\partial^2 W_2}{\partial y^2} + \frac{2vs^2}{C_{s2}^2}\varsigma W_2 - \frac{s^2}{C_{s2}^2}W_2 = 0 \end{cases}. \tag{7}$$

General solutions in the transform domain, which are bounded as $y \to \pm\infty$, can be expressed as

$$W_1 = P(s, \varsigma)e^{\beta_1(\varsigma)sy}, \quad y < 0, \tag{8}$$

$$W_2 = Q(s, \varsigma)e^{-\beta_2(\varsigma)sy}, \quad y > 0, \tag{9}$$

where the functions $P(s, \varsigma)$ and $Q(s, \varsigma)$ are to be determined by the boundary conditions and $\beta_i(\varsigma)$ are given by

$$\beta_i(\varsigma) = \sqrt{b_i + \varsigma(1 - b_i v)}\sqrt{b_i - \varsigma(1 + b_i v)} = \beta_{i+}(\varsigma)\beta_{i-}(\varsigma), \tag{10}$$

where

$$b_i = \frac{1}{C_{si}}, \quad i = 1, 2. \tag{11}$$

The displacements and shear stresses must be continuous across the interface, which gives the following conditions,

$$w_1(\xi, y = 0, t) = w_2(\xi, y = 0, t), \qquad 0 < \xi < \infty, \quad t > 0, \tag{12}$$

$$\tau_{yz1}(\xi, y = 0, t) = \tau_{yz2}(\xi, y = 0, t) = \tau_{yz}(\xi, 0, t), \quad 0 < \xi < \infty, \quad t > 0, \tag{13}$$

On the crack faces, there are

$$\tau_{yz1}(\xi, y = 0, t) = \tau_{yz2}(\xi, y = 0, t) = \tau_{yz}(\xi, 0, t) = -\dot{\tau}_0 t, \quad -\infty < \xi < 0, \quad t > 0. \tag{14}$$

Applying a one-sided Laplace transform with respect to time and a two-sided Laplace transform with respect to ξ on the shear stresses [20]

$$\hat{\tau}_{yzi}(\xi, y, s) = \int_0^\infty \tau_{yzi}(\xi, y, t)e^{-st}\mathrm{d}t, \tag{15}$$

$$T_{yzi}(\varsigma, y, s) = \int_{-\infty}^\infty \hat{\tau}_{yzi}(\xi, y, s)e^{-s\xi\varsigma}\mathrm{d}\xi, \tag{16}$$

and combining transforms in Eqs. 5 and 6 on the displacements, the boundary conditions (12–14) become

$$W_1(\varsigma, 0, s) = W_+ + \dot{\tau}_0 J_{1-}, \tag{17}$$

$$W_2(\varsigma, 0, s) = W_+ + \dot{\tau}_0 J_{2-}, \tag{18}$$

$$T_{yzi}(\varsigma, 0, s) = \frac{\dot{\tau}_0}{s^3\varsigma} + \dot{\tau}_0 H_+, \tag{19}$$

where

$$H_+ = \frac{1}{\dot{\tau}_0}\int_0^{\infty}\left[\int_0^{\infty}\tau_{yzi}(\xi > 0, 0, t)e^{-st}\mathrm{d}t\right]e^{-s\varsigma\xi}\mathrm{d}\xi, \tag{20}$$

$$J_{i-} = \frac{1}{\dot{\tau}_0}\int_{-\infty}^{0}\left[\int_0^{\infty}w_i(\xi < 0, 0, t)e^{-st}\mathrm{d}t\right]e^{-s\varsigma\xi}\mathrm{d}\xi. \tag{21}$$

In the transform domain, using the following relation,

$$T_{yzi}(\varsigma, 0, s) = \mu_i\frac{\partial W_i}{\partial y}\bigg|_{y=0} \tag{22}$$

yields

$$\begin{cases} Ps\beta_1(\varsigma)\mu_1 = \frac{\dot{\tau}_0}{s^3\varsigma} + \dot{\tau}_0 H_+ \\ -Qs\beta_2(\varsigma)\mu_2 = \frac{\dot{\tau}_0}{s^3\varsigma} + \dot{\tau}_0 H_+ \end{cases}. \tag{23}$$

In addition, Eqs. (8–9) and (17–18) lead to,

$$\begin{cases} P(\varsigma, 0, s) = W_+ + \dot{\tau}_0 J_{1-} \\ Q(\varsigma, 0, s) = W_+ + \dot{\tau}_0 J_{2-} \end{cases}. \tag{24}$$

Solving Eqs. 23 and 24, we obtain

$$P = \frac{\mu_2\beta_2(\varsigma)\dot{\tau}_0 J_-}{\mu_1\beta_1(\varsigma) + \mu_2\beta_2(\varsigma)}, \tag{25}$$

$$Q = \frac{-\mu_1\beta_1(\varsigma)\dot{\tau}_0 J_-}{\mu_1\beta_1(\varsigma) + \mu_2\beta_2(\varsigma)}, \tag{26}$$

where

$$J_- = J_{1-} - J_{2-}. \tag{27}$$

Substituting Eqs. 25 and 26 into Eq. 23, we have the following Wiener–Hopf equation,

$$J_- = \frac{\mu_1\beta_1(\varsigma) + \mu_2\beta_2(\varsigma)}{s\mu_1\mu_2\beta_1(\varsigma)\beta_2(\varsigma)}\left[\frac{1}{s^3\varsigma} + H_+\right], \tag{28}$$

At this point it is convenient to introduce a new function $R(\varsigma)$ by defining

$$R(\varsigma) = \frac{\mu_1\beta_1(\varsigma) + \mu_2\beta_2(\varsigma)}{\mu_1\mu_2 K\beta_2(\varsigma)}, \tag{29}$$

where

$$K = \frac{\mu_1\sqrt{1 - b_1^2v^2} + \mu_2\sqrt{1 - b_2^2v^2}}{\mu_1\mu_2\sqrt{1 - b_2^2v^2}}. \tag{30}$$

The Wiener–Hopf procedure requires $R(\varsigma)$ to be factored into the product of sectionally analytical functions

$$R(\varsigma) = R_+(\varsigma)R_-(\varsigma) \tag{31}$$

The function $R(\varsigma)$ has the properties that $R(\varsigma) \to 1$ as $|\varsigma| \to \infty$, and that $R(\varsigma)$ has neither zeros nor poles in the ς-plane with cuts along $-1/(C_{s1} - v) < \varsigma < -1/(C_{s2} - v)$ and $1/(C_{s2} + v) < \varsigma < 1/(C_{s1} + v)$.

The factorization of $R(\varsigma)$ begins by choosing two clockwise contours Γ_+ and Γ_- which embrace the branch cuts in the left and right half planes, respectively, followed by rewriting Eq. 31 as

$$\log R(\varsigma) = \log R_+(\varsigma) + \log R_-(\varsigma) = \frac{1}{2\pi i}\int_{\Gamma_+ + \Gamma_-} \frac{\log R(\eta)}{\eta - \varsigma} \mathrm{d}\eta, \tag{32}$$

with

$$\begin{aligned}
\log R_+(\varsigma) &= \frac{1}{2\pi i}\int_{\Gamma_+} \frac{\log R(\eta)}{\eta - \varsigma} \mathrm{d}\eta \\
&= \frac{1}{2\pi i}\left[\int_{-1/(C_{s2}-v)}^{-1/(C_{s1}-v)} \frac{\log R(\eta)}{\eta - \varsigma} \mathrm{d}\eta + \int_{-1/(C_{s1}-v)}^{-1/(C_{s2}-v)} \frac{\log R(\eta)}{\eta - \varsigma} \mathrm{d}\eta \right] \\
&= \frac{1}{2\pi i}\left[2i \int_{-1/(C_{s2}-v)}^{-1/(C_{s1}-v)} \frac{\mathrm{Im}\{\log R(\eta)\}}{\eta - \varsigma} \mathrm{d}\eta \right] \\
&= \frac{1}{\pi} \int_{1/(C_{s2}-v)}^{1/(C_{s1}-v)} \frac{\mathrm{Im}\{\log R(-\eta)\}}{\eta + \varsigma} \mathrm{d}\eta
\end{aligned} \tag{33}$$

and a similar expression for $\log R_-(\varsigma)$. These results lead to

$$R_+(\varsigma) = \exp\left\{ \frac{1}{\pi} \int_{1/(C_{s2}-v)}^{1/(C_{s1}-v)} \tan^{-1}\left[\frac{\mu_1 \beta_1(-\eta)}{\mu_2 |\beta_2(-\eta)|} \right] \frac{\mathrm{d}\eta}{\eta + \varsigma} \right\}, \tag{34}$$

and

$$R_-(\varsigma) = \exp\left\{ \frac{1}{\pi} \int_{1/(C_{s2}+v)}^{1/(C_{s1}+v)} \tan^{-1}\left[\frac{\mu_1 \beta_1(\eta)}{\mu_2 |\beta_2(\eta)|} \right] \frac{\mathrm{d}\eta}{\eta - \varsigma} \right\}. \tag{35}$$

In view of the previous discussion, Eq. 28 may be written as

$$J_- = \frac{K R_+(\varsigma) R_-(\varsigma)}{s\beta_{1+}(\varsigma)\beta_{1-}(\varsigma)} \left[\frac{1}{s^3 \varsigma} + H_+ \right], \tag{36}$$

then

$$\frac{J_- s\beta_{1-}(\varsigma)}{R_-(\varsigma)} - \left[\frac{K}{s^3 \varsigma} \frac{R_+(0)}{\beta_{1+}(0)} \right]_- = \left\{ \frac{K}{s^3 \varsigma} \left[\frac{R_+(\varsigma)}{\beta_{1+}(\varsigma)} - \frac{R_+(0)}{\beta_{1+}(0)} \right] \right\}_+ + \frac{K R_+(\varsigma)}{\beta_{1+}(\varsigma)} H_+. \tag{37}$$

The left-hand side of this equation is regular for $\mathrm{Re}(\varsigma) < 1/(C_{s2} + v)$, while the right-hand side is regular for $\mathrm{Re}(\varsigma) > -1/(C_{s2} - v)$. Applying the analytical continuation argument, therefore, each side of Eq. 34 represents one and the same entire function $E(\varsigma)$

$$\begin{aligned}
\frac{J_- s\beta_{1-}(\varsigma)}{R_-(\varsigma)} - \left[\frac{K}{s^3 \varsigma} \frac{R_+(0)}{\beta_{1+}(0)} \right]_- &= \left\{ \frac{K}{s^3 \varsigma} \left[\frac{R_+(\varsigma)}{\beta_{1+}(\varsigma)} - \frac{R_+(0)}{\beta_{1+}(0)} \right] \right\}_+ + \frac{K R_+(\varsigma)}{\beta_{1+}(\varsigma)} H_+ \\
&= k_0 + k_1 \varsigma + k_2 \varsigma^2 + \cdots + k_n \varsigma^n = E(\varsigma).
\end{aligned} \tag{38}$$

In order to ensure continuity of displacement when $\varsigma \to -\infty$, i.e. $\xi \to 0^-$ and vanishing of stresses when $\varsigma \to 0^+$, i.e., $\xi \to \infty$, we have

$$k_0 = k_1 = \cdots = k_n = 0, \tag{39}$$

which yields

$$J_- = \frac{K R_+(0) R_-(\varsigma)}{s^4 \varsigma \beta_{1+}(0) \beta_{1-}(\varsigma)} \tag{40}$$

and

$$H_+ = \frac{-1}{s^3 \varsigma} \left[1 - \frac{R_+(0)}{\beta_{1+}(0)} \frac{\beta_{1+}(\varsigma)}{R_+(\varsigma)} \right]. \tag{41}$$

Equations 15 and 20 show that the shear stress in the Laplace transform domain is

$$\hat{\tau}_{yz}(\xi, 0, s) = \frac{\dot{\tau}_0}{2\pi i} \int_L H_+ e^{s\varsigma\xi} \mathrm{d}(s\varsigma). \tag{42}$$

The corresponding stress intensity factor in the Laplace transform domain is

$$\hat{K}(s) = \lim_{\xi \to 0} \sqrt{2\pi\xi}\, \hat{\tau}_{yz}(\xi, 0, s) = \frac{\sqrt{2(1 - b_1 v)}\, \dot{\tau}_0 R_+(0)}{\beta_{1+}(0) s^{5/2}}. \tag{43}$$

Inverting the one-sided Laplace transform with respect to s, the stress intensity factor in (ξ, y, t) coordinate system can be obtained,

$$K(t) = \frac{4}{3} \dot{\tau}_0 R_+(0) \sqrt{\frac{2(1 - b_1 v) C_{s1} t^3}{\pi}}, \tag{44}$$

where $R_+(0)$ can be obtained from Eq. 34.

4 Solutions for a stationary crack

As mentioned in Sect. 2, the crack tip remains stationary until a critical time of initiation $t = t_{\text{init}}$. The dynamic deformation field of the stationary crack will be analyzed in this section.

The solutions can be obtained by substituting 0 for v in all the equations in Sect. 3, so that the corresponding stress intensity factor for the stationary crack can be expressed as

$$K(t) = \frac{4}{3} \dot{\tau}_0 R_+(0) \sqrt{\frac{2 C_{s1} t^3}{\pi}}, \tag{45}$$

where

$$R_+(0) = \exp\left\{ \frac{1}{\pi} \int_{1/C_{s2}}^{1/C_{s1}} \tan^{-1}\left[\frac{C_{s2}\mu_1 \sqrt{1 - C_{s1}^2 \eta^2}}{C_{s1}\mu_2 \left| \sqrt{1 - C_{s2}^2 \eta^2} \right|} \right] \frac{\mathrm{d}\eta}{\eta} \right\}. \tag{46}$$

The energy release rate for the stationary interface crack is

$$G = \frac{K^2(t)}{2\mu^*}, \tag{47}$$

where

$$\frac{2}{\mu^*} = \frac{1}{\mu_1} + \frac{1}{\mu_2}. \tag{48}$$

The Griffith criterion would predict that the crack tip will start to propagate when the crack tip energy release rate reaches the fracture energy of the interface, $\Delta\gamma$,

$$G = \Delta\gamma. \tag{49}$$

The critical time for crack initiation, at which the crack tip starts to move, is determined from Eqs. 47 and 49 as

$$t_{\text{init}} = \left[\frac{9\pi \mu^* \Delta\gamma}{16 C_{\text{s1}} \dot{\tau}_0^2 R_+^2(0)} \right]^{1/3}. \tag{50}$$

This predicts that the crack initiation time is proportional to the fracture energy via $\Delta\gamma^{1/3}$, and is inversely proportional to the applied loading rate via $\dot{\tau}_0^{2/3}$, which is also be found in [23] for interface crack initiation under in-plane shear and normal loading with constant stress rates.

For a homogeneous solid, i.e. $\mu_1 = \mu_2$, $C_{\text{s1}} = C_{\text{s2}} = C_{\text{s}}$, the stress intensity factor is

$$K(t) = \frac{4}{3} \dot{\tau}_0 \sqrt{\frac{2 C_{\text{s}} t^3}{\pi}}. \tag{51}$$

Using the Griffith criterion

$$G = 2\gamma \tag{52}$$

yields the crack initiation time

$$t_{\text{init}} = \left[\frac{9\pi \mu \gamma}{8 C_{\text{s}} \dot{\tau}_0^2} \right]^{1/3}, \tag{53}$$

where γ is the surface energy.

The shear stress ahead of the stationary crack tip in the Laplace transform domain can be obtained from Eq. 42 as

$$\hat{\tau}_{yz}(x > 0, 0, s) = \frac{\dot{\tau}_0}{\pi s^2} \int_{\frac{-1}{C_{\text{s2}}}}^{-\infty} \text{Im} \left\{ \frac{1}{\varsigma} \frac{R_+(0)}{\beta_{1+}(0)} \frac{\beta_{1+}(\varsigma)}{R_+(\varsigma)} \right\} e^{s\varsigma x} \text{d}\varsigma. \tag{54}$$

Assuming $\eta = -x\varsigma$,

$$\hat{\tau}_{yz}(x > 0, 0, s) = \frac{\dot{\tau}_0}{\pi s^2} \int_{\frac{x}{C_{\text{s2}}}}^{\infty} \frac{1}{\eta} \text{Im} \left\{ \frac{R_+(0)}{\beta_{1+}(0)} \frac{\beta_{1+}\left(-\frac{\eta}{x}\right)}{R_+\left(-\frac{\eta}{x}\right)} \right\} e^{-s\eta} \text{d}\eta. \tag{55}$$

Inverting the one-sided Laplace transform, we obtain the solutions of the shear stress ahead of the stationary crack tip as

$$\tau_{yz}^1(x > 0, 0, t) = \frac{\dot{\tau}_0}{\pi} \int_{\frac{x}{C_{\text{s2}}}}^{t} \frac{1}{\eta} \text{Im} \left\{ \left[\frac{R_+(0)}{\beta_{1+}(0)} \frac{\beta_1\left(-\frac{\eta}{x}\right) R_-\left(-\frac{\eta}{x}\right)}{\beta_{1-}\left(-\frac{\eta}{x}\right) R\left(-\frac{\eta}{x}\right)} \right] \right\} (t - \eta) \text{d}\eta H\left(t - \frac{x}{C_{\text{s2}}}\right), \tag{56}$$

where the superscript "1" of τ_{yz} denotes the first part of the result in the second sub-problem.

5 Transient solutions for a crack suddenly propagating at $t = t_{\text{init}}$

In this section, a transient analysis will be performed for a mode III crack suddenly propagating with a constant velocity v at time $t = t_{\text{init}}$. The constant loading rate $\dot{\tau}_0$ is imposed on the entire crack faces (including the new ones generated by crack propagation). Two cases are considered, one is $v < C_{\text{s1}}$ and another is $v = C_{\text{s1}}$. The moving coordinate ξ now is

$$\xi = x - v(t - t_{\text{init}}), \quad t > t_{\text{init}}, \tag{57}$$

where t is the total time and the governing equations of wave motions in the moving coordinates $\xi - y$ are the same as Eq. 3.

5.1 The case of $0 < v < C_{s1}$

In this case, we take t_1 as the time elapsed since the beginning of crack propagation, so that

$$t = t_1 + t_{\text{init}}, \quad t_1 > 0. \tag{58}$$

The corresponding boundary conditions on the interface are

$$w_1(\xi, y = 0, t_1) = w_2(\xi, y = 0, t_1), \quad 0 < \xi < \infty, \quad t_1 > 0, \tag{59}$$
$$\tau_{yz1}(\xi, y = 0, t_1) = \tau_{yz2}(\xi, y = 0, t_1), \quad 0 < \xi < \infty, \quad t_1 > 0 \tag{60}$$

and the tractions on the crack faces can be written as

$$\tau_{yzi}(\xi, y = 0, t_1) = -\dot{\tau}_0(t_1 + t_{\text{init}}), \quad -\infty < \xi < 0, \quad t_1 > 0, \quad i = 1, 2. \tag{61}$$

Using one-sided Laplace transform with respect to the time t_1 and two-sided Laplace transform with respect to ξ, the expressions for the displacement fields in the transform domain are the same as those in Eqs. 17 and 18. The stress fields in the transform domain become

$$T_{yzi}(\varsigma, 0, s) = \frac{\dot{\tau}_0}{s^3\varsigma} + \frac{\dot{\tau}_0 t_{\text{init}}}{s^2\varsigma} + \dot{\tau}_0 H_+, \tag{62}$$

where

$$H_+ = \frac{1}{\dot{\tau}_0}\int_0^\infty \left[\int_0^\infty \tau_{yzi}(\xi > 0, 0, t_1)e^{-st_1}\mathrm{d}t_1\right] e^{-s\varsigma\xi}\mathrm{d}\xi, \tag{63}$$

$$J_{i-} = \frac{1}{\dot{\tau}_0}\int_{-\infty}^0 \left[\int_0^\infty w_i(\xi < 0, 0, t_1)e^{-st_1}\mathrm{d}t_1\right] e^{-s\varsigma\xi}\mathrm{d}\xi. \tag{64}$$

Following the same method in Sect. 3, we obtain

$$J_- = \frac{K R_+(0)R_-(\varsigma)}{s^3\varsigma\beta_{1+}(0)\beta_{1-}(\varsigma)}\left(\frac{1}{s} + t_{\text{init}}\right), \tag{65}$$

$$H_+ = \frac{-1}{s^2\varsigma}\left(\frac{1}{s} + t_{\text{init}}\right)\left[1 - \frac{R_+(0)}{\beta_{1+}(0)}\frac{\beta_1(\varsigma)R_-(\varsigma)}{\beta_{1-}(\varsigma)R(\varsigma)}\right]. \tag{66}$$

As the moving crack tip propagates at a subsonic speed, the stress field has a singularity with exponent $-1/2$. The corresponding stress intensity factor in the Laplace transform domain is

$$\hat{K}(s) = \frac{\sqrt{2(1 - b_1 v)}\dot{\tau}_0 R_+(0)}{\beta_{1+}(0)\sqrt{s}}\left(\frac{1}{s^2} + \frac{t_{\text{init}}}{s}\right). \tag{67}$$

Inverting the one-sided Laplace transform with respect to s, the stress intensity factor in (ξ, y, t) coordinate system can be obtained,

$$K(t) = \left(\frac{4}{3}t_1^{\frac{3}{2}} + 2t_{\text{init}}t_1^{\frac{1}{2}}\right)\dot{\tau}_0 R_+(0)\sqrt{\frac{2(1 - b_1 v)C_{s1}}{\pi}}. \tag{68}$$

The shear stress ahead of the propagating crack tip in the Laplace transform domain can be obtained from Eqs. 42 and 66 as

$$\hat{\tau}_{yz}(\xi > 0, 0, s) = \frac{\dot{\tau}_0}{\pi}\left(\frac{1}{s^2} + \frac{t_{\text{init}}}{s}\right)\int_{\frac{-1}{C_{s2}-v}}^{-\infty} \mathrm{Im}\left\{\frac{1}{\varsigma}\frac{R_+(0)}{\beta_{1+}(0)}\frac{\beta_1(\varsigma)R_-(\varsigma)}{\beta_{1-}(\varsigma)R(\varsigma)}\right\} e^{s\varsigma\xi}\mathrm{d}\varsigma. \tag{69}$$

Assuming $\eta = -\xi\varsigma$, then

$$\hat{\tau}_{yz}(\xi > 0, 0, s) = \frac{\dot{\tau}_0}{\pi}\left(\frac{1}{s^2} + \frac{t_{\text{init}}}{s}\right) \int\limits_{\frac{\xi}{C_{s2}-v}}^{\infty} \frac{1}{\eta}\text{Im}\left\{\frac{R_+(0)}{\beta_{1+}(0)}\frac{\beta_{1+}\left(-\frac{\eta}{\xi}\right)}{R_+\left(-\frac{\eta}{\xi}\right)}\right\} e^{-s\eta}\text{d}\eta. \tag{70}$$

Inverting the one-sided Laplace transform with respect to s, we obtain the transient shear stress ahead of the crack tip as

$$\tau^2_{yz}(\xi > 0, 0, t) = \frac{\dot{\tau}_0}{\pi} \int\limits_{\frac{\xi}{C_{s2}-v}}^{t-t_{\text{init}}} \frac{1}{\eta}\text{Im}\left\{\frac{R_+(0)}{\beta_{1+}(0)}\frac{\beta_{1+}\left(-\frac{\eta}{\xi}\right)}{R_+\left(-\frac{\eta}{\xi}\right)}\right\}(t-\eta)\text{d}\eta H\left(t - t_{\text{init}} - \frac{\xi}{C_{s2}-v}\right), \tag{71}$$

where the superscript "2" of τ_{yz} denotes the second part of the result in the second sub-problem.

5.2 The case of $v = C_{s1}$

A critical velocity for a mode III interface crack is $v = C_{s1}$, at which the stress singularity vanishes and the energy release rate is zero. Gao et al. [23] used a combined atomistic-continuum approach to investigate a mode II dominated intersonic crack in a homogeneous material and showed that, as the crack propagates at the Rayleigh wave speed, the stress singularity vanishes but the shear stress exhibits a very sharp peak ahead of the moving crack tip, which facilitates the nucleation of an intersonic daughter crack. Here, we analyze if a peak stress would emerge as a mode III crack begins to move at the lower shear wave speed of the two materials.

For the transient velocity $v = C_{s1}$, Eq. 10 becomes

$$\beta_1(\varsigma) = \sqrt{b_1}\sqrt{b_1 - 2\varsigma} = \sqrt{b_1}\beta_{1-}(\varsigma), \tag{72}$$

$$\beta_2(\varsigma) = \sqrt{b_2 + \varsigma(1 - b_2C_{s1})}\sqrt{b_2 - \varsigma(1 + b_2C_{s1})} = \beta_{2+}(\varsigma)\beta_{2-}(\varsigma). \tag{73}$$

Using the same method as in previous sections, the final Wiener-de Hoop equation can be expressed as

$$J_- = \frac{\mu_1\beta_1(\varsigma) + \mu_2\beta_2(\varsigma)}{s\mu_1\mu_2\beta_1(\varsigma)\beta_2(\varsigma)}\left[\frac{1}{s^3\varsigma} + \frac{t_{\text{init}}}{s^2\varsigma} + H_+\right]. \tag{74}$$

Substituting Eqs. 72 and 73 into Eq. 74 yields

$$s\mu_1\sqrt{b_1}\beta_{1-}(\varsigma)J_- = \frac{\mu_1\beta_1(\varsigma) + \mu_2\beta_2(\varsigma)}{\mu_2\beta_2(\varsigma)}\left[\frac{1}{s^3\varsigma} + \frac{t_{\text{init}}}{s^2\varsigma} + H_+\right]. \tag{75}$$

Corresponding to Eq. 29, in this case $R(\varsigma)$ is introduced as

$$R(\varsigma) = \frac{\mu_1\beta_1(\varsigma) + \mu_2\beta_2(\varsigma)}{\mu_2\beta_2(\varsigma)} = 1 + \frac{\mu_1\beta_1(\varsigma)}{\mu_2\beta_2(\varsigma)}. \tag{76}$$

which can be factorized into two regular functions $R_+(\varsigma)$ and $R_-(\varsigma)$ as

$$R_+(\varsigma) = \exp\left\{\frac{1}{\pi}\int\limits_{1/(C_{s2}-C_{s1})}^{\infty} \tan^{-1}\left[\frac{\mu_1\beta_1(-\eta)}{\mu_2\,|\beta_2(-\eta)|}\right]\frac{\text{d}\eta}{\eta + \varsigma}\right\}, \tag{77}$$

$$R_-(\varsigma) = \exp\left\{\frac{1}{\pi}\int\limits_{1/(C_{s2}+C_{s1})}^{1/(2C_{s1})} \tan^{-1}\left[\frac{\mu_1\beta_1(\eta)}{\mu_2\,|\beta_2(\eta)|}\right]\frac{\text{d}\eta}{\eta - \varsigma}\right\}. \tag{78}$$

We then obtain

$$J_- = \frac{R_+(0)R_-(\varsigma)}{s\mu_1\sqrt{b_1}\beta_{1-}(\varsigma)}\left(\frac{1}{s^3\varsigma}+\frac{t_{\text{init}}}{s^2\varsigma}\right), \tag{79}$$

$$H_+ = -\left(\frac{1}{s^3\varsigma}+\frac{t_{\text{init}}}{s^2\varsigma}\right)\left[1-\frac{R_+(0)R_-(\varsigma)}{R(\varsigma)}\right]. \tag{80}$$

Equations (79–80) can also be obtained from Eqs. 65 and 66 by inserting $v = C_{s1}$.

As $\xi \to 0$, the shear stress in the Laplace transform domain

$$\hat{\tau}_{yz}(\xi \to 0, 0, s) = -\dot{\tau}_0\left(\frac{1}{s^2}+\frac{t_{\text{init}}}{s}\right)(1-R_+(0)) \tag{81}$$

yields

$$K(t) = 0, \tag{82}$$

which means that the singularity of the stress field ahead of the moving crack tip vanishes when the velocity of the crack tip attains the lower shear wave speed of the two materials.

Using the inverse of two-sided Laplace transformation, we obtain

$$\hat{\tau}_{yz}(\xi > 0, 0, s) = \frac{\dot{\tau}_0}{\pi}\left(\frac{1}{s^2}+\frac{t_{\text{init}}}{s}\right)\int\limits_{\frac{\xi}{C_{s2}-C_{s1}}}^{\infty}\frac{1}{\eta}\text{Im}\left\{\frac{R_+(0)R_-\left(-\frac{\eta}{\xi}\right)}{R\left(-\frac{\eta}{\xi}\right)}\right\}e^{-s\eta}\text{d}\eta. \tag{83}$$

Inverting the one-sided Laplace transform with respect to s, the shear stress ahead of the crack tip can be written as

$$\tau_{yz}^2 = \frac{\dot{\tau}_0}{\pi}\int\limits_{\frac{1}{C_{s2}-C_{s1}}}^{\frac{t-t_{\text{init}}}{\xi}}\frac{1}{r}\text{Im}\left\{\frac{R_+(0)R_-(-r)}{R(-r)}\right\}(t-r\xi)\text{d}r\,H\left(\frac{t-t_{\text{init}}}{\xi}-\frac{1}{C_{s2}-C_{s1}}\right), \tag{84}$$

where the superscript "2" of τ_{yz} denotes the second part of the result in the second sub-problem.

6 The total shear stress ahead of the moving crack tip

As mentioned in Sect. 2, the original problem consists of two sub-problems. For the second sub-problem, the diffracted waves include two parts: the first one is induced from the stationary crack tip and the second one is generated from the propagating crack tip as the crack starts to move. In Sects. 4 and 5, we have obtained the shear stress fields ahead of the crack tip, respectively, so that the total shear stress ahead of the crack tip for $t > t_{\text{init}}$ can be obtained as follows.

6.1 The case of $v < C_{s1}$

For the case of $v < C_{s1}$, the total shear stress ahead of the crack tip is the sum of the uniform shear stress in Eq. 1 from the first sub-problem and the non-uniform shear stress from the second sub-problem stated above,

$$\sigma_{yz}(\xi > 0, 0, t) = \dot{\tau}_0 t + \tau_{yz}^1 + \tau_{yz}^2, \quad t > t_{\text{init}}, \tag{85}$$

where τ_{yz}^1 can be obtained from Sect. 4, in which $v = 0$, as

$$\tau_{yz}^1 = \frac{\dot{\tau}_0}{\pi}\int\limits_{\max\left[\frac{1}{C_{s2}},\frac{t-t_{\text{init}}}{\xi+v(t-t_{\text{init}})}\right]}^{\frac{t}{\xi+v(t-t_{\text{init}})}}\frac{1}{r}\text{Im}\left\{\frac{R_+(0)}{\beta_{1+}(0)}\frac{\beta_{1+}(-r)}{R_+(-r)}\right\}[t-r\xi-rv(t-t_{\text{init}})]\text{d}r$$
$$\times H\left[\frac{t}{\xi+v(t-t_{\text{init}})}-\frac{1}{C_{s2}}\right] \tag{86}$$

and τ_{yz}^2 has been obtained in Sect. 5.1, in which $0 < v < C_{s1}$

$$\tau_{yz}^2 = \frac{\dot{\tau}_0}{\pi} \int_{\frac{1}{C_{s2}-v}}^{\frac{t-t_{\text{init}}}{\xi}} \frac{1}{r} \text{Im} \left\{ \frac{R_+(0)}{\beta_{1+}(0)} \frac{\beta_{1+}(-r)}{R_+(-r)} \right\} (t - r\xi) \text{d}r \, H \left(\frac{t - t_{\text{init}}}{\xi} - \frac{1}{C_{s2} - v} \right), \tag{87}$$

it should be noted that $R(\varsigma)$ and $\beta(\varsigma)$ in Eqs. 86 and 87 correspond to the cases of $v = 0$ and $0 < v < C_{s1}$, respectively.

6.2 The case of $v = C_{s1}$

For the case of $v = C_{s1}$, the total shear stress ahead of the crack tip is

$$\tau_{yz}^T(\xi > 0, 0, t) = \dot{\tau}_0 t + \tau_{yz}^1 + \tau_{yz}^2, \quad t > t_{\text{init}}, \tag{88}$$

where

$$\tau_{yz}^1 = \frac{\dot{\tau}_0}{\pi} \int_{\max\left[\frac{1}{C_{s2}}, \frac{t-t_{\text{init}}}{\xi + C_{s1}(t-t_{\text{init}})}\right]}^{\frac{t}{\xi + C_{s1}(t-t_{\text{init}})}} \frac{1}{r} \text{Im} \left\{ \frac{R_+(0)}{\beta_{1+}(0)} \frac{\beta_{1+}(-r)}{R_+(-r)} \right\} [t - r\xi - rC_{s1}(t - t_{\text{init}})] \text{d}r \times H \left[\frac{t}{\xi + C_{s1}(t - t_{\text{init}})} - \frac{1}{C_{s2}} \right] \tag{89}$$

and

$$\tau_{yz}^2 = \frac{\dot{\tau}_0}{\pi} \int_{\frac{1}{C_{s2}-C_{s1}}}^{\frac{t-t_{\text{init}}}{\xi}} \frac{1}{r} \text{Im} \left\{ \frac{R_+(0) R_-(-r)}{R(-r)} \right\} (t - r\xi) \text{d}r \, H \left(\frac{t - t_{\text{init}}}{\xi} - \frac{1}{C_{s2} - C_{s1}} \right), \tag{90}$$

$R(\varsigma)$ and $\beta(\varsigma)$ in Eqs. 89 and 90 correspond to the cases of $v = 0$ and $v = C_{s1}$, respectively.

7 Numerical results and predictions

From the above analysis, one can see that the stress field ahead of the moving crack tip is singular when $v < C_{s1}$ and the singularity vanishes when $v = C_{s1}$. The total shear stresses are shown in Eqs. 85–87 and 88–90, respectively. Numerical methods are used to calculate the stress distributions ahead of the crack tip.

The shear stress distribution ahead of the moving crack tip in Eqs. 85–87 for $v = 0.8C_{s1}$ is shown in Fig. 3 at five times the initiation time for crack propagation, i.e., $t = 5t_{\text{init}}$ and $C_{s1}/C_{s2} = 0.5$, where the shear stress is normalized by the loading rate $\dot{\tau}_0$ and the initiation time t_{init}, and the distance $\xi > 0$ to the moving crack tip is normalized by the lower shear wave speed C_{s1} and t_{init}. It is clearly observed that the shear stress is singular near the crack tip.

Equations 88–90 for the shear stress distribution ahead of the moving crack tip for $v = C_{s1}$ is shown in Fig. 4 at five times the initiation time for crack propagation, i.e., $t = 5t_{\text{init}}$ and $C_{s1}/C_{s2} = 0.5$, where the shear stress is also normalized by the loading rate $\dot{\tau}_0$ and the initiation time t_{init}, and the distance $\xi > 0$ to the moving crack tip is normalized by the lower shear wave speed C_{s1} and t_{init}. It is clearly observed that the singularity vanishes but the shear stress has a peak ahead of the crack tip. In fact, it can be shown from Eqs. 88–90 that, for any time $t > t_{\text{init}}$, the peak always occurs at some distance ahead of the moving crack tip. Similar to Gao et al. [23], it can be expected that a daughter crack would emerge at the position of the peak when the peak value attains the theoretical strength of the interface and a faster crack supersonic with respect to the soft medium should be found under this situation.

From numerical calculation, we find that the relationship between the normalized shear stress $\tau_{yz}/(\dot{\tau}_0 t_{\text{init}})$ and the normalized distance $\xi/(C_{s1}t_{\text{init}})$ only depends on two ratios, i.e., C_{s1}/C_{s2} and t/t_{init}. Compared to the

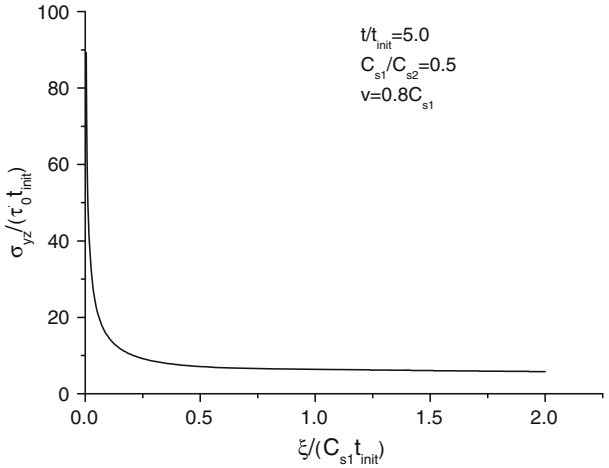

Fig. 3 Distribution of the normalized shear stress $\sigma_{yz}/(\dot{\tau}_0 t_{\text{init}})$ ahead of the propagating interfacial crack tip as a function of the normalized distance $\xi/(C_{\text{s1}} t_{\text{init}})$ from the crack tip for the case of $t = 5t_{\text{init}}$, $C_{\text{s1}}/C_{\text{s2}} = 0.5$ and $v = 0.8C_{\text{s1}}$. Singularity in the stress field is shown near the crack tip

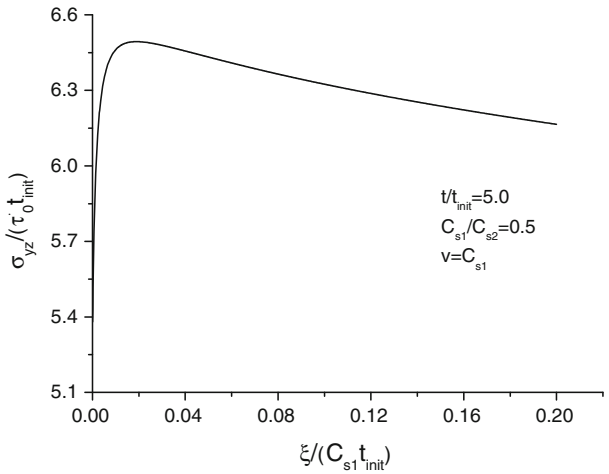

Fig. 4 Distribution of the normalized shear stress $\sigma_{yz}/(\dot{\tau}_0 t_{\text{init}})$ ahead of the propagating interface crack tip as a function of the normalized distance $\xi/(C_{\text{s1}} t_{\text{init}})$ from the crack tip for the case of $t = 5t_{\text{init}}$, $C_{\text{s1}}/C_{\text{s2}} = 0.5$ and $v = C_{\text{s1}}$. Note that singularity in the stress field vanishes, but a peak emerges at a distance ahead of the crack tip

case of a mode II crack moving at the Rayleigh wave speed in a homogeneous material [23], in which the peak stress always occurs at the shear wave front, the peak stress in the present case should occur at the front of an interface wave.

When the ratio of shear wave speeds of the two materials are known, we can find the position of the peak stress ahead of the crack tip at any time $t > t_{\text{init}}$. Figure 5 shows the normalized position of the peak $\xi/(C_{\text{s1}} t_{\text{init}})$ for different ratios $C_{\text{s1}}/C_{\text{s2}}$ at time $t = 5t_{\text{init}}$. One can see that the relationship between the position of the peak and the ratio $C_{\text{s1}}/C_{\text{s2}}$ is nonlinear. As $C_{\text{s1}}/C_{\text{s2}}$ tends to be one, i.e., a homogeneous case, the position of the peak approaches to the crack tip, which means supersonic propagation will not occur for a mode III crack in a homogeneous material (at least within the linear elastic framework). Generally speaking, the smaller the ratio $C_{\text{s1}}/C_{\text{s2}}$, the farther the peak stress emerges away from the moving crack tip.

Figure 6 shows curves of the normalized shear stress distributions $\tau_{yz}/(\dot{\tau}_0 t_{\text{init}})$ ahead of the moving crack tip via the normalized distance $\xi/(C_{\text{s1}} t_{\text{init}})$ from the crack tip, for three different ratios $C_{\text{s1}}/C_{\text{s2}}$ at time $t = 5t_{\text{init}}$. One can see that, in the region of (0,1], the larger the ratio $C_{\text{s1}}/C_{\text{s2}}$, the larger the peak stress ahead of the crack tip.

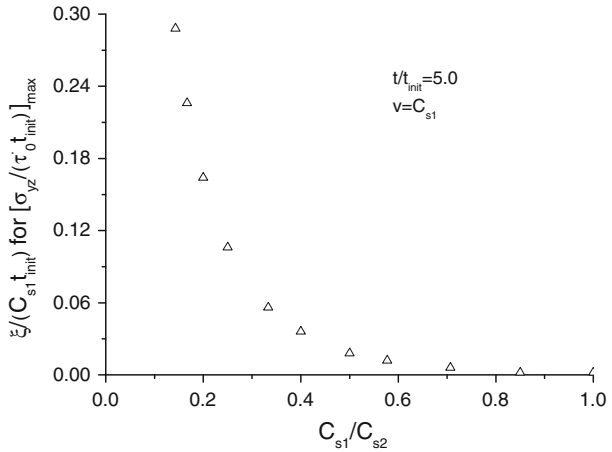

Fig. 5 The normalized position of the peak stress for different ratios of shear wave speeds C_{s1}/C_{s2} of the two materials at time $t = 5t_{init}$ and the propagation velocity $v = C_{s1}$. Nonlinear relationship is shown between the speed of the interface wave and the ratios of shear wave speeds C_{s1}/C_{s2}

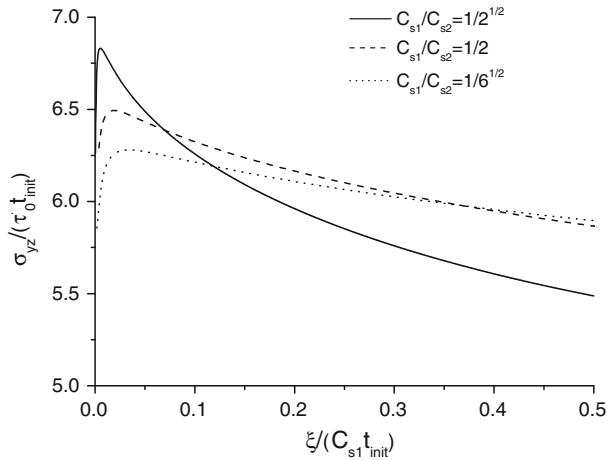

Fig. 6 Distributions of the normalized shear stress $\sigma_{yz}/(\dot{\tau}_0 t_{init})$ ahead of the propagating interface crack tip as a function of the normalized distance $\xi/(C_{s1}t_{init})$ from the crack tip at time $t = 5t_{init}$ and velocity $v = C_{s1}$, for three different ratios of shear wave speeds C_{s1}/C_{s2}

8 Further discussions

The present study, along with the previous studies on crack motion along biomaterial interfaces, indicates that the limiting speed of crack motion is determined by the stiff material of the system, even though the soft material can impose one or a number of velocity barriers to reach that limiting speed. Whenever the crack reaches a velocity barrier, a stress peak develops ahead of the crack and, when it reaches the limiting strength of the material, a supersonic daughter crack forms at the location of the peak stress, overcoming the velocity barrier. This process can be repeated if there exist more than one velocity barriers, as demonstrated by Buehler and Gao [10].

We would like to point out that the above description of crack motion is limited to linear elastic materials. In nonlinear or inelastic materials, supersonic cracks can exist even in homogeneous materials. Indeed, molecular dynamics simulation [3–5] and experiments [45] have shown both super-Rayleigh mode I crack motion and supersonic mode II crack motion. In order to explain the observed supersonic crack motion, Buehler et al. [12] and Buehler and Gao [11] performed atomistic simulations to show that hyperelasticity, the elasticity at large strains, plays a crucial role in supersonic fracture by dominating crack behavior when the size of the hyperelastic region approaches a characteristic length scale associated with local energy flow near the crack tip. The study of Buehler et al. [12] provides a strong support for an earlier hypothesis made by Gao [21,22]

and Abraham [1] that hyperelastic effects at the crack tip could govern the dynamic behaviors of a crack and change the limiting speed of cracks by enhancing or reducing local energy flow. Marder [44,45] pointed out that inelastic dissipation could also give rise to super-Rayleigh or supersonic fracture. Guo et al. [28] analyzed a mode III crack in steady-state motion and showed that the possible existence of supersonic fracture relies on two conditions: the upturn stress–strain relation and sufficient pre-stress. Guozden and Jagla [29] found supersonic motion of a mode III crack in a lattice model with elastic stiffening at large deformation. These studies have fundamentally expanded our understanding of the limiting crack speeds beyond linear elastic theories of solids. We do not pursue more details here.

Acknowledgments This study was initiated when both authors were working at the Max Planck Institute for Metals Research. Financial supports from the Chang Jiang Scholar Program through the Ministry of Education of China, NSFC (Grant No. 10972220, 10732050, and 10721202) and the key project of CAS through Grant KJCX2-YW-M04 are also gratefully acknowledged.

References

1. Abraham, F.F.: Dynamics of brittle fracture with variable elasticity. Phys. Rev. Lett. **77**, 272–275 (1996)
2. Abraham, F.F., Brodbeck, D., Rudge, W.E., Xu, X.: A molecular-dynamics investigation of rapid fracture mechanics. J. Mech. Phys. Solids **45**, 1595–1619 (1997)
3. Abraham, F.F., Gao, H.: How fast can cracks propagate? Phys. Rev. Lett. **84**, 3113–3116 (2000)
4. Abraham, F.F., Walkup, R., Gao, H. et al.: Simulating materials failure by using up to one billion atoms and the world's fastest computer: brittle fracture. Proc. Natl. Acad. Sci. USA **99**, 5777–5782 (2002)
5. Abraham, F.F., Walkup, R., Gao, H. et al.: Simulating materials failure by using up to one billion atoms and the world's fastest computer: work-hardening. Proc. Natl. Acad. Sci. USA **99**, 5783–5787 (2002)
6. Andrews, D.J.: Rupture velocity of plane strain shear cracks. J. Geophys. Res. **81**, 5679–5687 (1976)
7. Broberg, K.B.: The near-tip field at high crack velocities. Int. J. Fract. **39**, 1–13 (1989)
8. Broberg, K.B.: Intersonic crack propagation in an orthotropic material. Int. J. Fract. **99**, 1–11 (1999)
9. Buehler, M.J.: Atomistic and continuum studies of deformation and failure in brittle solids and thin film systems. Ph. D. Dissertation, Max-Planck Institute for Metals Research (2004)
10. Buehler, M.J., Gao, H.: A mother–daughter–granddaughter mechanism of shear dominated intersonic crack motion along interfaces of dissimilar materials. J. Chin. Inst. Eng. **27**(6), 763–769 (2004)
11. Buehler, M.J., Gao, H.: Dynamical fracture instabilities due to local hyperelasticity at crack tips. Nature **439**, 307–310 (2006)
12. Buehler, M.J., Abraham, F.F., Gao, H.: Hyperelasticity governs dynamic fracture at a critical length scale. Nature **426**, 141–146 (2003)
13. Burridge, R.: Admissible speeds for plane strain shear cracks with friction but lacking cohesion. Geophys. J. R. Soc. Lond. **35**, 439–455 (1973)
14. Chen, B., Huang, Y., Gao, H., Wu, P.: Shear crack propagation along weak planes in solids: a finite deformation analysis incorporating the linear harmonic potential. Int. J. Solids Struct. **41**, 1–14 (2004)
15. Chen, B., Huang, Y., Gao, H., Yang, W.: On the finite opening of intersonic shear crack. Int. J. Solids Struct. **41**, 2293–2306 (2004)
16. Coker, D., Rosakis, A.J.: Experimental observations of intersonic crack growth in asymmetrically loaded unidirectional composite plates. Philos. Mag. A **81**, 571–595 (2001)
17. Deng, X.: Transient, asymptotic, elastodynamic analysis: a simple method and its application to mixed-mode crack growth. Int. J. Solids Struct. **30**, 513–519 (1993)
18. Fineberg, J., Marder, M.: Instability in dynamic fracture. Phys. Rep. Rev. Sect. Phys. Lett. **313**, 2–108 (1999)
19. Freund, L.B.: The mechanics of dynamics shear crack propagation. J. Geophys. Res. **84**, 2199–2209 (1979)
20. Freund, L.B.: Dynamic fracture mechanics. Cambridge University Press, Cambridge (1990)
21. Gao, H.: A theory of local limiting speed in dynamic fracture. J. Mech. Phys. Solids **44**, 1453–1474 (1996)
22. Gao, H.: Elastic waves in a hyperelastic solid near its plane-strain equibiaxial cohesive limit. Philos. Mag. Lett. **76**, 307–314 (1997)
23. Gao, H., Huang, Y., Abraham, F.F.: Continuum and atomistic studies of intersonic crack propagation. J. Mech. Phys. Solids **49**, 2113–2132 (2001)
24. Gao, H., Chen, S.H., Buehler, M.J.: Dynamic crack propagation in a heterogeneous material strip: study of the Broberg problem by continuum and atomistic methods. In: The 11th International Conference of Fracture (ICF11), Turin (Italy), March 20–25 (2005)
25. Geubelle, P.H., Kubair, D.: Intersonic crack propagation in homogeneous media under shear dominated loading: numerical analysis. J. Mech. Phys. Solids **49**, 571–587 (2001)
26. Guo, G.F., Yang, W., Huang, Y., Rosakis, A.J.: Suddenly decelerating or accelerating intersonic shear cracks. J. Mech. Phys. Solids **51**, 311–331 (2003)
27. Guo, G.F., Yang, W., Huang, Y.: Intersonic crack growth under time dependent loading. Int. J. Solids Structure **40**, 2757–2765 (2003)
28. Guo, G.F., Yang, W., Huang, Y.: Supersonic crack growth in a solid of upturn stress–strain relation under anti-plane shear. J. Mech. Phys. Solids **51**, 1971–1985 (2003)
29. Guozden, T.M. Jagla: Supersonic crack propagation in a class of lattice models of mode III brittle fracture. Phys. Rev. Lett. **95**, 224302 (2005)

30. Huang, Y., Liu, C., Rosakis, A.J.: Transonic crack growth along a bimaterial interface: an investigation of the asymptotic structure of near-tip fields. Int. J. Solids Struct. **33**, 2625–2645 (1996)
31. Huang, Y., Wang, W., Liu, C., Rosakis, A.J.: Analysis of intersonic crack growth in unidirectional fiber-reinforced composites. J. Mech. Phys. Solids **47**, 1893–1916 (1999)
32. Huang, Y., Gao, H.: Intersonic crack propagation. Part I: the fundamental solution. J. Appl. Mech. **68**, 169–175 (2001)
33. Huang, Y., Gao, H.: Intersonic crack propagation. Part II: suddenly stopping crack. J. Appl. Mech. **69**, 76–80 (2002)
34. Ing, Y., Ma, C.: Transient analysis of a subsonic propagating interface crack subjected to antiplane dynamic loading in dissimilar isotropic materials. J. Appl. Mech. **64**, 546–556 (1997)
35. Ing, Y., Ma, C.: Dynamic analysis of a propagating antiplane interface crack. J. Eng. Mech. **123**, 783–791 (1997)
36. Koizumi, H., Kirchner, H.O.K., Suzuki, T.: Lattice wave emission from moving cracks. Philos. Mag. **87**, 4093–4107 (2007)
37. Koizumi, H., Kirchner, H.O.K., Suzuki, T.: Supersonic crack motion in a harmoni lattice. Philos. Mag. Lett. **87**, 589–593 (2007)
38. Kostrov, B.V.: On the crack propagation with variable velocity. Int. J. Fract. **11**, 47–56 (1975)
39. Kubair, D.V., Geubelle, P.H., Huang, Y.: Intersonic crack propagation in homogeneous media under shear-dominated loading: theoretical analysis. J. Mech. Phys. Solids **50**, 1547–1564 (2002)
40. Kubair, D.V., Geubelle, P.H., Huang, Y.: Analysis of a rate-dependent cohesive model for dynamic crack propagation. Eng. Fract. Mech. **50**, 685–704 (2003)
41. Kulamekhtova, S.A., Saraikin, V.A., Slepyan, L.I.: Plane problem of a crack in a lattice. Mech. Solids **19**, 101–108 (1984)
42. Liu, C., Lambros, J., Rosakis, A.J.: Highly transient elastodynamic crack growth in a bimaterial interface: hogher order asymptotic analysis and experiments. J. Mech. Phys. Solids **41**, 1887–1954 (1993)
43. Ma, C.C., Ing, Y.S.: Transient analysis of dynamic crack propagation with boundary effect. J. Appl. Mech. **62**, 1029–1038 (1995)
44. Marder, M.: Shock-wave theory for rupture of rubber. Phys. Rev. Lett. **94**, 048001 (2005)
45. Marder, M.: Supersonic rupture of rubber. J. Mech. Phys. Solids **54**, 491–532 (2006)
46. Mishuris, G.S., Movchan, A.B., Slepyan, L.I.: Dynamical extraction of a single chain from a discrete lattice. J. Mech. Phys. Solids **56**, 487–495 (2008)
47. Needleman, A.: An analysis of intersonic crack growth under shear loading. ASME J. Appl. Mech. **66**, 847–857 (1999)
48. Needleman, A., Rosakis, A.J.: The e.ect of bond strength and loading rate on the conditions governing the attainment of intersonic crack growth along interfaces. J. Mech. Phys. Solids **47**, 2411–2449 (1999)
49. Rosakis, A.J.: Intersonic crack propagation in bimaterial systems. J. Mech. Phys. Solids **46**, 1789–1813 (1998)
50. Rosakis, A.J., Samudrala, O., Coker, D.: Cracks faster than the shear wave speed. Science **284**, 1337–1340 (1999)
51. Rosakis, A.J.: Intersonic shear cracks and fault ruptures. Adv. Phys. **51**, 1189–1257 (2002)
52. Samudrala, O., Huang, Y., Rosakis, A.J.: Subsonic and intersonic mode II crack propagation with a rate dependent cohesive zone. J. Mech. Phys. Solids **50**, 1231–1268 (2002)
53. Samudrala, O., Huang, Y., Rosakis, A.J.: Subsonic and intersonic shear rupture of weak planes with a velocity weakening cohesive zone. J. Geophys. Res. Solid Earth **107**(B8), (2002b). doi:10.1029/2001JB000460
54. Simonov, I.V.: Behavior of solutions of dynamic problems in the neighborhood of the edge of a cut moving at transonic speed in an elastic medium. Mech. Solids **18**, 100–106 (1983)
55. Slepyan, L.I.: Dynamics of brittle fracture in lattice. Doklady Sov. Phys. **26**, 538–540 (1981)
56. Slepyan, L.I.: Dynamic factor in impact, phase transition and fracture. J. Mech. Phys. Solids **48**, 927–960 (2000)
57. Slepyan, L.I.: Feeding and dissipative waves in fracture and phase transition II. Phase-transition waves. J. Mech. Phys. Solids **49**, 513–550 (2001)
58. Slepyan, L.I., Ayzenberg-Stepanenko, M.V.: Some surprising phenomena in weak-bond fracture of a triangular lattice. J. Mech. Phys. Solids **50**, 1591–1625 (2002)
59. Slepyan, L.I., Ayzenberg-Stepanenko, M.V.: Localized transition waves in bistable-bond lattices. J. Mech. Phys. Solids **52**, 1447–1479 (2004)
60. Wang, W., Huang, Y., Rosakis, A.J., Liu, C.: Effect of elastic mismatch in intersonic crack propagation along a bimaterial interface. Eng. Fract. Mech. **61**, 471–485 (1998)
61. Yu, H.H., Yang, W.: Mechanics of transonic debonding of a bimaterial interface: the anti-plane shear case. J. Mech. Phys. Solids **42**, 1789–1802 (1994)
62. Yu, H.H., Suo, Z.: Intersonic crack growth on an interface. Proc. R. Soc. Lond. A **456**, 23–246 (2000)
63. Zhu, J.J., Kuang, Z.B.: On interface crack propagation with variable velocity for logitudinal shear problem. Int. J. Fract. **72**, 121–144 (1995)